[9]W. Heitler, *The Quantum Theory of Radiation* (Oxford U. P., Oxford, England, 1954), 3rd ed.

[10]Such operators are known from the many-body treatment of excitons. See, e.g., H. Haken, Fortsch. Physik 6, 271 (1958); H. Haken and W. Schottky, Z. Phys. Chem. (Frankfort) 16, 3 (1958); R. S. Knox, *Theory of Excitons* (Academic, New York, 1963).

[11]The $\vec{k}$ selection rule reads

$$\sum_j e^{i(\vec{k}'+\vec{q}-\vec{k})\vec{R}_j} \neq 0 \text{ if } \begin{cases} \vec{k}'+\vec{q}-\vec{k}=0, & \text{normal processes} \\ \vec{k}'+\vec{q}-\vec{K}_j, & \text{umklapp processes} \end{cases}$$

where $\vec{R}_j$ and $\vec{K}_j$ are lattice and reduced reciprocal-lattice vectors, respectively. We neglect umklapp processes, and write

$$\sum_j e^{i(\vec{k}'+\vec{q}-\vec{k})\vec{R}_j} = N\delta_{\vec{k}'+\vec{q},\vec{k}} .$$

[12]In addition to Ref. 10 see, for instance, H. Haken, Phys. Chem. Solids 8, 166 (1959); Z. Physik 155, 223 (1959); Y. Takeuti, Progr. Theoret Phys. (Kyoto) 18, 421 (1957).

[13]C. Horie, Progr. Theoret Phys. (Kyoto) 21, 113 (1959).

[14]A representation of the plasmon ground state by electron-hole-pair states was given by M. Lang, thesis, Stuttgart 1964 (unpublished).

[15]N. N. Bogolyubov, Zh. Eksperim. i Teor. Fiz. 34, 58 (1958) [Soviet Phys. JETP 7, 41 (1958)]; N. N. Bogolyubov, V. V. Tolmacher, and D. V. Shirkov, *New Method in the Theory of Superconductivity* (Consultants Bureau, New York, 1959).

[16]This simplification is compatible with the time-reversal properties (1.28).

[17]See for instance P. Nozières and D. Pines, Phys. Rev. 109, 741 (1958); 109, 1062 (1958).

[18]Though the wave vector $\vec{q}$ remains a good quantum number in our polariton representation, we have to distinguish between the two energy levels.

[19]Based on Ovander's (Ref. 3) research, a similar treatment of fourth-order nonlinearities in molecular crystals was given by B. S. Toshich, Fiz. Tverd. Tela 9, 4713 (1967) [Soviet Phys. Solid State 9, 1346 (1967)].

[20]R. C. C. Leite and S. P. S. Porto, Phys. Rev. Letters 17, 10 (1966); R. C. C. Leite and J. F. Scott, *ibid.* 22, 130 (1969); R. C. C. Leite, J. F. Scott, and T. C. Damen, *ibid.* 22, 780 (1969); M. Klein and S. P. S. Porto, *ibid.* 22, 782 (1969); J. F. Scott, R. C. C. Leite, and T. C. Damen, Phys. Rev. 188, 1285 (1969).

[21]A. Pinczuk and E. Burstein, Phys. Rev. Letters 21, 1073 (1968).

[22]D. C. Hamilton, Phys. Rev. 188, 1221 (1969).

[23]D. G. Thomas and J. J. Hopfield, Phys. Rev. 175, 1021 (1968); J. J. Hopfield, *ibid.* 182, 945 (1969).

[24]E. Burstein, D. L. Mills, A. Pinczuk, and S. Ushioda, Phys. Rev. Letters 22, 348 (1969); D. L. Mills and E. Burstein, Phys. Rev. 188, 1465 (1969).

[25]C. K. N. Patel and R. E. Slusher, Phys. Rev. Letters 21, 1563 (1968); Phys. Rev. 167, 413 (1968); Phys. Rev. Letters 22, 282 (1969).

[26]P. A. Wolff, Phys. Rev. Letters 16, 225 (1966); P. M. Platzman, N. Tzoar, and P. A. Wolf, Phys. Rev. 174, 489 (1968); E-Ni Foo and N. Tzoar, *ibid.* 184, 644 (1969); P. A. Wolff, Phys. Rev. B 1, 950 (1970).

PHYSICAL REVIEW B VOLUME 2, NUMBER 10 15 NOVEMBER 1970

Electron Mobility in II-VI Semiconductors

D. L. Rode
Bell Telephone Laboratories, Murray Hill, New Jersey 07974
(Received 17 June 1970)

The electron drift mobility in CdS, CdSe, CdTe, ZnS, ZnSe, and ZnTe is calculated by an iterative solution of the Boltzmann equation for lattice scattering. Piezoelectric, deformation-potential acoustic-mode, and polar-mode scattering are included. The acoustic deformation potential appropriate to acoustic-mode scattering appears to be much higher than previously expected.

I. INTRODUCTION

The electron mobility in II-VI compound semiconductors can be understood by a consideration of the scattering of conduction electrons by fundamental lattice vibrations.[1] Although impurity scattering[2,3] is also well known, this mechanism does not contribute to the lattice mobility. Its effect in commonly pure materials is negligible at temperatures above ~100 °K. The theory of electron scattering by lattice vibrations[4,5] is exceptionally accurate for isotropic direct-gap materials because of our knowledge of the conduction-band structure.[6] By an iterative solution of the Boltzmann equation,[7,8] the electron mobility follows exactly from the assumed model described below. The wurtzitelike and zinc-blende-like crystals CdS, CdSe, CdTe, ZnS, ZnSe, and ZnTe, being wide-gap semiconductors, are especially well suited to calculation and are the only materials discussed here. The direct-gap III-V semiconductors have been discussed previously.[8]

There are five main conclusions evident from the present work. First, the three scattering mechanisms discussed by several authors[1,9,10] are sufficient to predict the lattice mobility, i.e., polar-mode scattering,[5] acoustic mode via deformation-potential coupling,[11] and acoustic mode via piezoelectric coupling.[12] Second, Matthiessen's rule[13] (reciprocal mobility is the sum of reciprocal component mobili-

ties due to each scattering mechanism acting alone) is accurate to ~15%. Third, the nonparabolicity of the conduction band is fairly unimportant, lowering the mobility in CdTe at 500 °K by only ~15%. Fourth, the effect of the temperature dependence of the low-frequency dielectric constant[1,9] is largely offset by a similar variation of the high-frequency dielectric constant[14] which has been previously ignored. Thus, both dielectric constants are assumed, to good approximation, to be temperature independent. This assumption still leaves one with large discrepancies between experiment and theory at high temperatures.[9,15] The discrepancies, however, disappear upon the use of larger acoustic deformation potentials than those calculated by an earlier method.[4] Conduction-band nonparabolicity[6] removes only a small part of the difference. The fifth conclusion is then that acoustic deformation potentials are larger and the corresponding component mobilities are an order of magnitude lower than those calculated earlier. Hot-electron experiments[16] in CdS support this result.

II. BAND STRUCTURE AND SCATTERING MECHANISMS

Only a brief presentation of the band-structure model is required here since the details can be found elsewhere.[6,8] The six crystals mentioned earlier can be acquired with the cubic zinc-blende structure.[17] However, it is common that CdS and CdSe have the hexagonal wurtzite structure[18] and these two crystals will be considered to have the wurtzite structure for the remainder of this paper. The only clear indication of mobility anisotropy in the uniaxial wurtzite structure occurs at low temperatures in pure crystals[19] and can be fairly well explained in terms of the piezoelectric stress tensor (whose anisotropy we do retain) rather than by anisotropy in the effective mass.[12] In any case, the conduction band is nearly spherical[20] and is assumed to be so here. The results of Kane[6] can then be used along with the approximation that spin-orbit splitting vanishes. The latter is an accurate assumption for GaAs (a III-V semiconductor) and an even better assumption for the wide-gap II-VI semiconductors.[8]

The electron effective mass at the conduction-band edge m^* is somewhat increased to that of the polaron as described by Frohlich.[21] Because of the ionic nature of the lattice, the electron induces a virtual polar phonon about itself which lowers the electron energy and gives rise to a free carrier, called a polaron, whose mass exceeds the effective mass. The coupling is weak. Only about 0.2–0.3 virtual phonons are typically present, and the corresponding mass increase is less than ~10% (see Table I). Since the polaron energy should approach the effective-mass energy as the crystal momentum $\hbar k$ becomes large because coupling to the phonon field weakens, we would expect the polaron perturbation energy to decrease for sufficiently large k. Frohlich's[21] formulation applies to electrons in parabolic bands and to electron energies less than the polar-phonon energy whereas our present interest includes many electrons with higher as well as lower energies. Therefore, the electron effective mass calculated from Kane's band-structure theory by Kurik[20] will be used exclusive of the polaron effect. To estimate the effect due to polaron coupling, the coupling constant[21] α ($\approx 2\times$the number of virtual phonons[22]) is calculated (see Table I):

$$\alpha = (\kappa_0 - \kappa_\infty)\frac{(e^4 m^*/2\hbar^3\omega_{po})^{1/2}}{\kappa_0\kappa_\infty}\ , \qquad (1)$$

where κ_0 and κ_∞ are, respectively, the low- and high-frequency relative dielectric constants and $\hbar\omega_{po}$ is the polar optical-phonon energy. At $\vec{k}=0$, the polaron mass[21] is $m_p = m^*/(1-\frac{1}{6}\alpha)$.

The scattering rate due to polar modes[8,21] is proportional to α which depends sensitively upon the relatively small difference between the dielectric constants. The low-frequency dielectric constant is known to be temperature dependent[1] and this dependence has been shown by Segall *et al.*[15] to reduce considerably the electron mobility in CdTe above room temperature if the high-frequency dielectric constant indeed remains constant. One cannot, evidently, neglect the temperature dependence of κ_∞.[14] In general, the temperature coefficient of mobility due to polar-mode scattering is proportional to $\partial \ln\alpha/\partial T$ and can be related simply to the temperature coefficients of κ_0 and κ_∞: $\partial \ln\kappa_0/\partial T$ and $\partial \ln\kappa_\infty/\partial T$. Assuming m^* and ω_{po} to be constant, Eq. (1) yields

$$\frac{\partial \ln\alpha}{\partial T} = \left(\frac{\kappa_\infty\,\partial \ln\kappa_0}{\partial T} - \frac{\kappa_0\,\partial \ln\kappa_\infty}{\partial T}\right)\Big/(\kappa_0-\kappa_\infty). \qquad (2)$$

For CdTe,[15] $\partial \ln\kappa_0/\partial T \approx 2.3\times10^{-4}/\,^\circ\mathrm{K}$ so that $\partial \ln\alpha/\partial T \approx 6.8\times10^{-4}/\,^\circ\mathrm{K}$ if κ_∞ is constant (see Table I). However, between 300 and 500 °K we find[14] that $\partial \ln\kappa_\infty/\partial T \approx 0.9\times10^{-4}/\,^\circ\mathrm{K}$ so that $\partial \ln\alpha/\partial T$ is only about $3.2\times10^{-4}/\,^\circ\mathrm{K}$. Similarly for CdS, we find that the respective values of $\partial \ln\alpha/\partial T$ for[14,23] $\partial \ln\kappa_\infty/\partial T = 0$ and $1.4\times10^{-4}/\,^\circ\mathrm{K}$ are $\pm 1.7\times10^{-4}/^\circ\mathrm{K}$. One finds similar behavior in the III-V semiconductor GaAs where $\partial \ln\kappa_0/\partial T$ and $\partial \ln\kappa_\infty/\partial T$ are accurately known.[8] These results suggest that the simplified Lyddane-Sachs-Teller relation ($\kappa_0/\kappa_\infty = \omega_{po}^2/\omega_t^2$, where $\hbar\omega_t$ is the energy of the transverse polar optical phonon at the center of the Brillouin zone) is accurate to a fraction of 1%, as is expected, and that temperature-dependent dielectric constants alone cannot bring the calculated mobility into agreement with experiment. Hence, we assume that κ_0 and κ_∞ are constant since their temperature

dependences are not known in detail and probably cancel to the present order of approximation.

From the foregoing model, the scattering terms of the Boltzmann equation can be reduced exactly, as shown previously for the zinc-blende structure.[8] The only necessary modifications to Ref. 8 are due to the wurtzite structure. Specifically, there is no change in the formulation regarding polar-mode scattering. For deformation-potential acoustic-mode scattering, the spherically averaged elastic stiffness constant c_l (see Table I) must be related to four independent elastic constants c_{ij} as shown by Zook,[12]

$$c_l = \tfrac{1}{3}(2c_{11} + c_{33}) - \tfrac{2}{15} c_x \quad , \tag{3}$$

where

$$c_x = c_{11} + c_{33} - 2c_{13} - 4c_{44} \quad . \tag{4}$$

For piezoelectric scattering in the zinc-blende structure, there is only one independent element of the piezoelectric tensor, denoted earlier[8] as e_{14}/ϵ_0, where ϵ_0 is the low-frequency dielectric permittiv-

TABLE I. Material parameters at 300 °K.

Material	CdS (set I)	CdS (set II)	CdSe
Structure	Wurtzite	Wurtzite	Wurtzite
Effective mass, m^*/m	0.165 (Ref. 20)	(Use m_p of set I)	0.131 (Ref. 20)
Polaron mass, m_p/m	0.180		0.142
Coupling constant, α	0.56		0.48
Effective-mass energy gap, E_g^* (eV) (Refs. 1 and a)	2.52	Same	1.77
Low-frequency relative dielectric constant, $\mathcal{K}_0$	8.60[b]	9.19 (Ref. 18)	9.40[b]
High-frequency relative dielectric constant, $\mathcal{K}_\infty$	5.31[b]	5.19 (Ref. 18)	6.10[b]
Polar-phonon equivalent temperature, T_{po} (°K)	433[b]	Same	304[b]
Acoustic deformation potential, E_1 (eV)	14.5 (Ref. 16)	Same	11.5[c]
Longitudinal acoustic-mode elastic stiffness constant, c_l (10^{10} N/m^2) (Ref. 12)	8.95	Same	7.40
Transverse acoustic-mode elastic stiffness constant, c_t (10^{10} N/m^2) (Ref. 12)	1.90	Same	1.72
Piezoelectric tensor elements			
h_x (10^9 V/m) (Ref. 12)	13.4	(1.40 × set-I	8.95
h_{15} (10^9 V/m) (Ref. 12)	−2.63	data for $\mu_\parallel$ and	−1.77
h_{33} (10^9 V/m) (Ref. 12)	5.21	1.53 × set-I data	3.84
h_{14} (19^9 V/m) (Ref. 12)		for $\mu_\perp$)	

Material	CdTe	ZnS	ZnSe	ZnTe
Structure	Zinc blende	Zinc blende	Zinc blende	Zinc blende
m^*/m	0.111[d]	0.230 (Ref. 20)	0.180 (Ref. 20)	0.151[d]
m_p/m	0.117	0.254	0.193	0.159
α	0.30	0.64	0.43	0.30
E_g^* (Refs. 1 and a)	1.54	3.77	2.78	2.34
$\mathcal{K}_0$	9.65[b]	8.32 (Ref. 1)	8.33[e]	9.67[b]
$\mathcal{K}_\infty$	7.21[b]	5.13 (Ref. 1)	5.90[e]	7.28[b]
T_{po}	246 (Ref. 1)	507[e]	360[b]	297[e]
E_1	9.5[c]	14.5[c]	11.5[f]	9.5[c]
c_l (Ref. 12)	6.97	12.89	10.34	8.41
c_t (Ref. 12)	1.55	3.60	3.29	2.48
h_x (Ref. 12)				
h_{15} (Ref. 12)				
h_{33} (Ref. 12)				
h_{14} (Ref. 12)	0.394	2.26	0.61	0.314

[a] R. E. Halsted, in Ref. 1.
[b] M. Balkanski, in Ref. 10.
[c] Extrapolated from E_1 for CdS and ZnSe.
[d] Extrapolated from Ref. 20.
[e] S. Ushioda, A. Pinczuk, W. Taylor, and E. Burstein, in Ref. 10.
[f] Fitted to high-temperature mobility data of Ref. 25.

ity. In the wurtzite structure, the quantity $e_{14}^2/\rho\epsilon_0^2 u_p^2$ in Ref. 8 must be replaced by $h_\perp^2/\rho u_p^2$ and $h_\parallel^2/\rho u_p^2$ which, respectively, apply to drift mobilities measured perpendicular and parallel to the c axis of the crystal. These spherically averaged coupling constants include scattering by the longitudinal electric fields of longitudinal and transverse acoustic modes.[12] There are now three independent elements h_{ij} (see Table I) of the piezoelectric tensor and (Zook,[12] for isotropic effective mass) the coupling constants are

$$\frac{h_\perp^2}{\rho u_p^2} = 4h_{15}^2 \frac{21 + 6h_x/h_{15} + h_x^2/h_{15}^2}{105c_t} + h_{33}^2 \frac{21 - 24h_x/h_{33} + 8h_x^2/h_{33}^2}{105c_l} \tag{5}$$

and

$$\frac{h_\parallel^2}{\rho u_p^2} = 2h_{15}^2 \frac{21 + 18h_x/h_{15} + 5h_x^2/h_{15}^2}{105c_t} + h_{33}^2 \frac{63 - 36h_x/h_{33} + 8h_x^2/h_{33}^2}{105c_l} , \tag{6}$$

where

$$c_t = c_{44} + \tfrac{2}{15} c_x \tag{7}$$

and

$$h_x = h_{33} - h_{31} - 2h_{15} . \tag{8}$$

When the foregoing results are applied to the scattering terms presented in Ref. 8, the finite difference equation which yields the electron distribution function perturbed by a small electric field can be solved numerically as before by iteration. The low-field drift mobility of electrons is then calculated from the perturbation distribution function. Results are presented and compared with experiment in Sec. III.

III. DRIFT MOBILITY

Material parameters necessary for calculating mobility are shown in Table I. Only theoretical values of the effective mass are used. The electron effective mass in CdS, CdSe, ZnS, and ZnSe has been calculated by Kurik[20] and determined for CdTe and ZnTe by extrapolation. An isotropic effective mass m^* where

$$1/m^* = \tfrac{1}{3}(1/m_\parallel^* + 2/m_\perp^*) \tag{9}$$

is used in the calculations and tabulated in Table I. The effective-mass energy gap[4] E_g^* at room temperature is calculated from the optical gap E_g by

$$E_g^*(300\,^\circ\mathrm{K}) = \tfrac{2}{3} E_g(0\,^\circ\mathrm{K}) + \tfrac{1}{3} E_g(300\,^\circ\mathrm{K}),$$

which is approximately true.[4] Values for E_g^* directly affect nonparabolicity, which should be accurate to about 1% in mobility. Where the dielectric permittivities are anisotropic, the isotropic value

$$\epsilon = \tfrac{1}{3}(\epsilon_\parallel + 2\epsilon_\perp) \tag{10}$$

is used for the calculation. The remaining parameters with the exception of E_1, can be found in the indicated references and in the foregoing discussion. Deformation potentials E_1 have been extrapolated from hot-electron experiments[16] on CdS and high-temperature mobility data[24, 24a] on CdSe and ZnSe (see below).

A. CdS: Wurtzite Structure

Figure 1 shows the calculated drift mobility of CdS compared to experimental Hall mobility.[19, 25, 26] All of the experimental data in this paper are Hall mobilities for which the Hall factor is not accurately known, although the correction therefrom ($\lesssim 20\%$) is within the uncertainty of the calculation due to inaccuracies in the assumed material parameters. This particular sample[10, 19] of CdS is the only semiconductor thus far observed to exhibit a monotonic negative temperature coefficient down to 2 °K. Ordinarily, impurity scattering dominates at low temperatures. Thus, CdS presents a nearly ideal mobility curve suitable for studying piezoelectric scattering which becomes dominant at low temperatures (as indicated by the mobility[8] $\mu \sim 1/T^{1/2}$ dependence). Polar-mode scattering dominates above 100 °K where the mobility is isotropic to within experimental error.[19] The portion of the curves

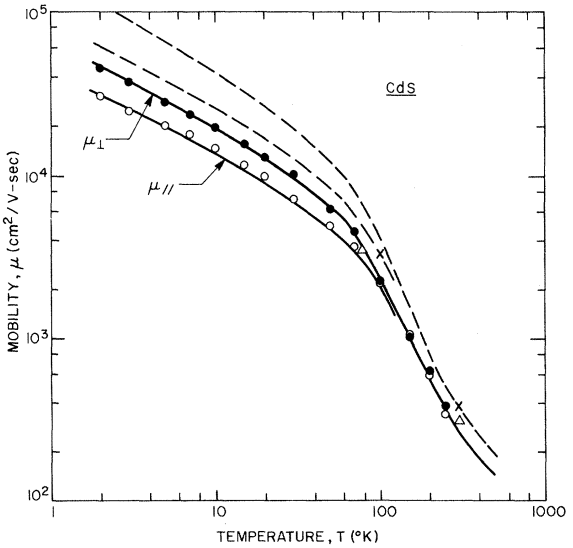

FIG. 1. Electron mobility in CdS. Data points from Refs. 19 (○, ●), 26 (X), and 27 (Δ) represent Hall mobilities. Dashed curves are calculated from set-I parameters in Table I. Solid curves are calculated from set-II parameters in Table I with readjusted piezoelectric constants. Note the large range of temperature.

around 80 °K is equally affected by piezoelectric, deformation-potential acoustic, and polar-mode scattering for the deformation potential $E_1 = 14.5$ eV listed in Table I. From the formula[4]

$$E_1 = -\left(\frac{\partial E_g}{\partial P}\right)_T \Big/ K \ , \qquad (11)$$

where K is the compressibility, one finds $E_1 = 2.9$ eV, but Kobayashi[10] has shown this value to be much too small to explain the experimental mobility. Saitoh[16] finds $E_1 = 16 \pm 2$ eV from a hot-electron experiment, and we have found $E_1 = 14.5$ eV to fit the observed mobility as shown in Fig. 1.

The data (circles) at low temperatures display the expected anisotropy due mainly to the piezoelectric tensor. A more accurate estimate of the ratio $\mu_\perp/\mu_\parallel$ can be obtained by including the effective-mass anisotropy as Zook[12] has done. The dashed curves were calculated from CdS parameters in Table I labeled set I. The solid curves were calculated from set-II parameters and indicate the typical uncertainty of the present results above 100 °K. The low-temperature data were fitted to the solid curves by increasing the piezoelectric tensor elements by factors of 1.53 for $\mu_\perp$ and 1.40 for $\mu_\parallel$. By correctly including mass anisotropy in the piezoelectric coupling constants these factors could be made nearly equal, but the reason for the discrepancy between the low-temperature data and the dashed curves remains unexplained since Berlincourt *et al.*[18] measured the h_{ij} to within a few percent accuracy. It seems unlikely that a combination of impurity-scattering mechanisms[2,3] could conspire to maintain the $1/T^{1/2}$ dependence.

In any case, these data show that one need not quantize the acoustic-phonon distribution even at these low temperatures since, if this were the case, the mobility would decrease faster than $1/T^{1/2}$ as T increases. The equipartition assumption is expected to be valid if the electron velocity v is much greater than twice the sound speed μ. At 2.0 °K in Fig. 1, this condition is barely satisfied ($v \approx 4\mu$). Furthermore, Eq. (11) evidently is not reliable for estimating the deformation potential. The mobility due to deformation-potential scattering is proportional to[8] $1/E_1^2$ and is lower than that predicted by Eq. (11) by the factor $(14.5/2.9)^2 = 25$.

Figure 2 demonstrates the accuracy of Matthiessen's rule[13,27] applied to CdS for deformation-potential acoustic-mode, piezoelectric, and polar-mode scattering. The respective mobilities μ_{ac}, μ_{po}, and μ_{pe} due to each mechanism acting alone were calculated by the iterative technique[8] and are shown in Fig. 2. Kohler[28] has shown that μ_M represents an upper limit for the total mobility μ, i.e.,

$$1/\mu_M = 1/\mu_{ac} + 1/\mu_{po} + 1/\mu_{pe} \leq 1/\mu \ , \qquad (12)$$

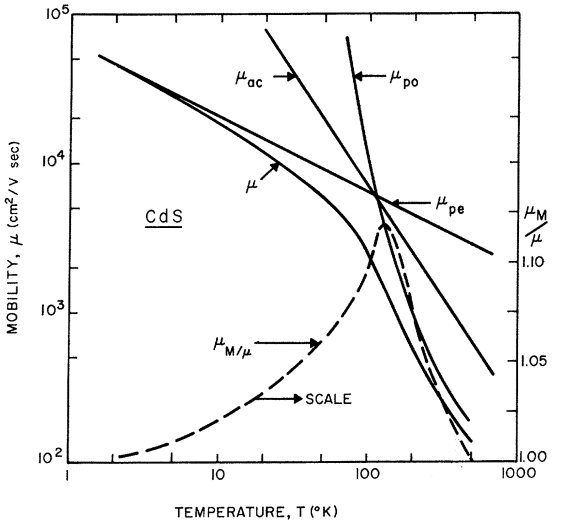

FIG. 2. Electron mobility calculated from Matthiessen's rule μ_M compared to actual mobility μ. μ_{ac} is deformation-potential acoustic mode, μ_{pe} is piezoelectric, and μ_{po} is polar-mode scattering limited mobility.

and μ_M/μ should be near unity when one scattering mechanism dominates all others. This occurs for piezoelectric scattering at low temperatures and for polar-mode scattering at high temperatures in Fig. 2, where, indeed, μ_M/μ approaches unity. Even near 140 °K, where all three scattering mechanisms are comparable, Eq. (12) is seen to be rather accurate, $\mu_M/\mu \approx 1.12$.

It will be helpful for the reader to keep in mind the relative magnitudes and trends of $\mu_{pe}(\sim 1/T^{1/2})$, $\mu_{ac}(\sim 1/T^{3/2})$, and μ_{po} appearing in Fig. 2 for all the direct-gap polar semiconductors as they are all similar. In particular, the slight positive curvature of μ_{po} at higher temperatures will eventually allow μ_{ac} to become nearly as small as μ_{po} at elevated temperatures. Hence, the acoustic deformation potential E_1 can strongly influence mobility results for $T \gtrsim 1000$ °K.

B. CdSe: Wurtzite Structure

The mobility of CdSe shown in Fig. 3 for conduction parallel or perpendicular to the c axis of the crystal resembles that of CdS, Fig. 1. Experimental data[1,24a,29,30] on sufficiently pure material which would confirm the predicted anisotropy have not been attained. Impurity scattering tends to limit the experimental mobilities shown in Fig. 3 below 60 °K. At higher temperatures where lattice-limited mobilities are observed, the agreement is satisfactory for the extrapolated deformation potential $E_1 = 11.5$ shown in Table I, which is that found for ZnSe by fitting high-temperature mobility data (see below).

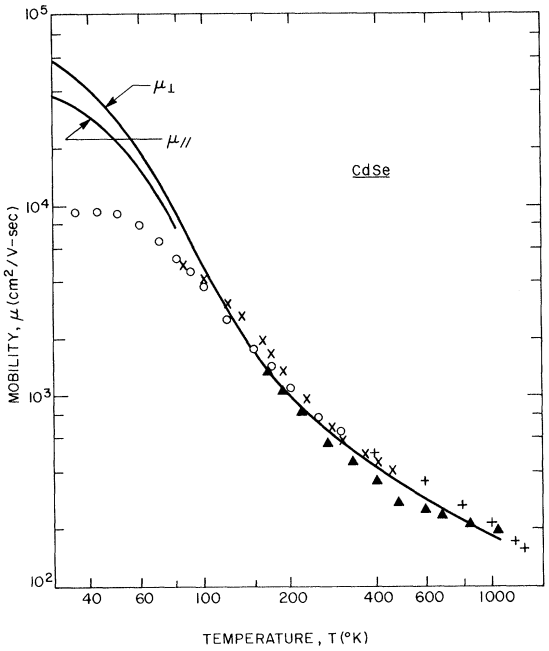

FIG. 3. Electron mobility in CdSe. Data points from Refs. 30 (○), 1 (X), 24 (+), 31 (▲). Solid curves are calculated from parameters in Table I. Agreement is satisfactory over more than an order of magnitude in temperature. Impurity scattering limits the low-temperature experimental mobility so that the data do not show the predicted anisotropy.

C. CdTe: Zinc-Blende Structure

Figure 4 shows the mobility[15,31,32] of CdTe calculated for the zinc-blende structure. The relatively low experimental mobilities[15] (data circles) below 60 °K are again due to impurity scattering. From 60 to 600 °K, the agreement is reasonable for the purer sample measured by Segall *et al.*[15] In Fig. 7 of their work, they have achieved agreement between theory and experiment nearly as good as that shown in the present Fig. 4 by assuming a temperature-dependent $\mathcal{K}_0$. $\mathcal{K}_\infty$ was considered constant. However, from our discussion of Sec. II it appears that $\mathcal{K}_0$ *and* $\mathcal{K}_\infty$ can be consistently considered constant to the present approximation. The previous disagreement[15] between theory and experiment is then removed by the use of a larger deformation potential E_1 than that predicted by Eq. (11). E_1 = 9.5 eV, as shown in Table I, was extrapolated from the results on CdS and CdSe. At temperatures greater than 700 °K, the high-temperature mobility data of Smith[32] fall well below the dashed curve in Fig. 4. This difference cannot be suitably removed by readjustments of the deformation potential and is probably due to simultaneous conduction in higher-lying ⟨111⟩ minima which are a few tenths of an eV above the (0, 0, 0) valley.[33]

CdTe has the smallest energy gap of the six materials being considered and should therefore exhibit the largest effect due to conduction-band nonparabolicity. Figure 5 compares the mobility in parabolic and nonparabolic bands. The effective mass $m^* = 0.111$ in either case, and the curves at temperatures greater than 700 °K are illustrative only since multivalley conduction sets in at this point. At 500 °K, nonparabolicity lowers the mobility by only about 15%.

D. ZnS and ZnTe: Zinc-Blende Structure

ZnS in sufficiently pure form for mobility studies is not generally available.[1] The data[34–36] shown in Fig. 6 may be limited by impurity scattering even at room temperature. However, several authors do find similar 300 °K mobility values which are much lower than the predicted value 285 cm^2/V sec. Some reported values are 140,[35] 165,[37] 142,[36] and 160 cm^2/V sec[37] (this last value is reported for a hexagonal structure and the crystal may have been contaminated with Cd). Lenz (quoted in Ref. 35) has, however, found a value of 285 cm^2/V sec, which agrees with the predicted value. A detailed

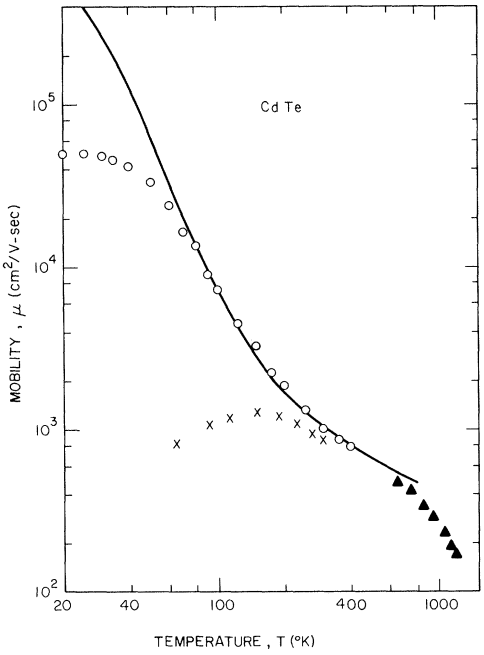

FIG. 4. Electron mobility in CdTe. Data points from Refs. 15 (○), 32 (X), 33 (▲). Solid curve is calculated from parameters in Table I for the zinc-blende structure. Impurity scattering is evident below 60 °K for the ○ data and below 200 °K for the X data. The rapid decrease above 700 °K of the ▲ data suggests multivalley conduction.

explanation for the discrepancy in Fig. 6 is not presently available.

ZnTe ordinarily (however, see Ref. 1) exhibits p-type conduction and a detailed comparison with the predicted electron mobility shown in Fig. 7 must await measurements on pure material.

E. ZnSe: Zinc-Blende Structure

The mobility in ZnSe,[9,24,38] shown in Fig. 8 as a solid curve, follows from the parameters in Table I. The dashed line corresponds to a lower deformation potential $E_1 = 2.4$ eV derived from Eq. (11). At low temperatures, below 150 °K, the experimental mobility[38] is dominated by impurity scattering. For intermediate temperatures, in the neighborhood of room temperature, the agreement with either theoretical curve is satisfactory. But at elevated temperatures, greater than 600 °K, the agreement not only in absolute magnitude but also in functional dependence is seen to be much better

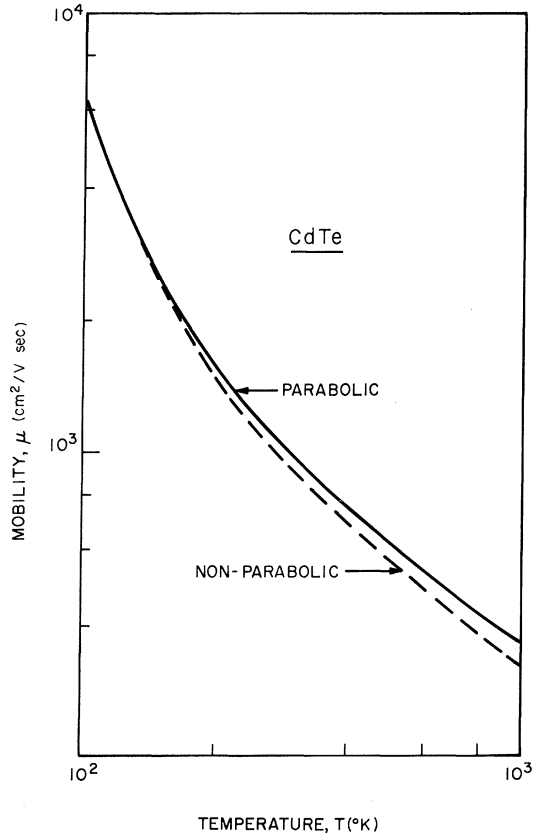

FIG. 5. Electron mobility in CdTe calculated for a parabolic conduction-band valley and compared to that for the correct nonparabolic band. The parabolic model always predicts a higher mobility and is in error by 15% at 500 °K.

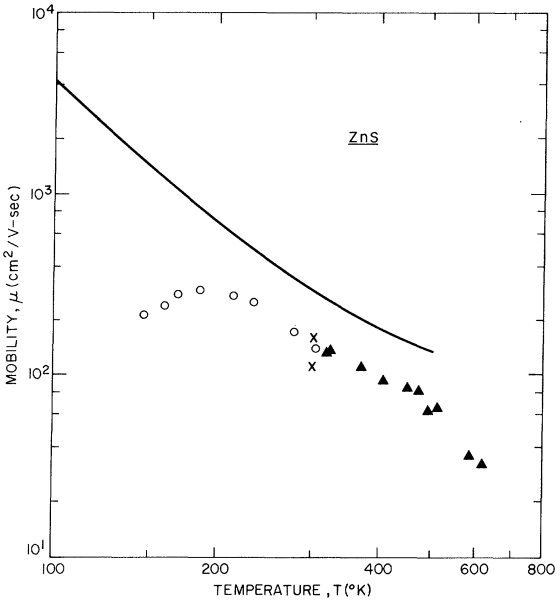

FIG. 6. Electron mobility in ZnS. Data points from Refs. 36 (○), 37 (X), and 35 (▲) are probably limited by impurities to values well below the solid curve calculated from parameters in Table I.

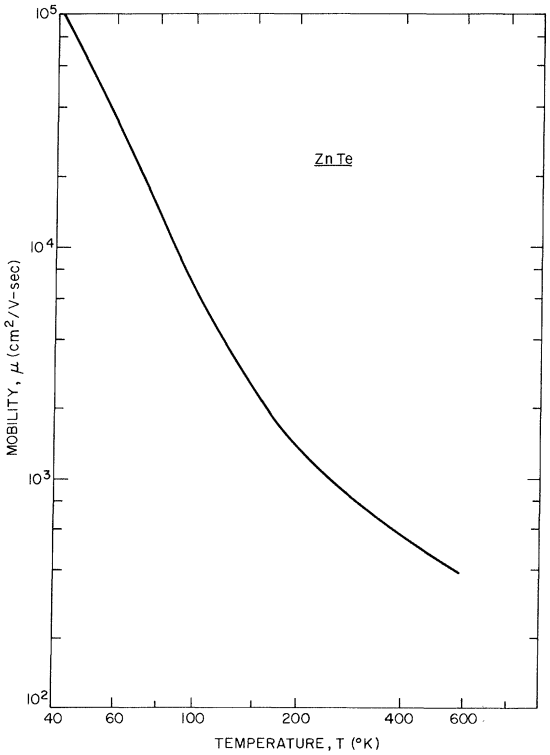

FIG. 7. Electron mobility in ZnTe. Extensive mobility data are not yet available on ZnTe which ordinarily exhibits p-type conduction.

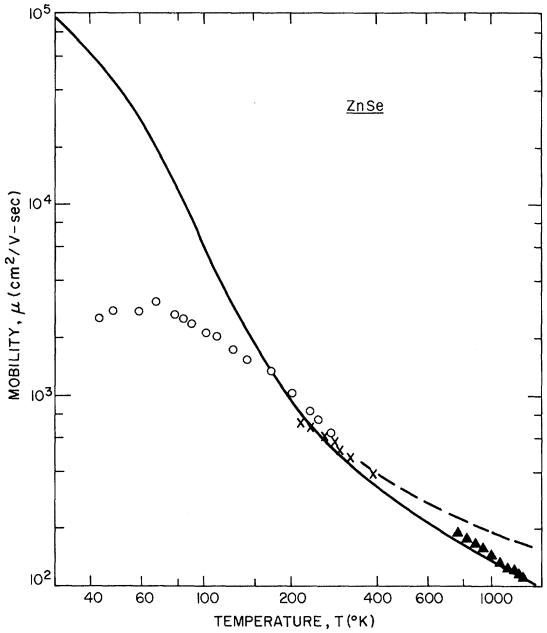

FIG. 8. Electron mobility in ZnSe. Data points from Refs. 39 (○), 9 (X), and 25 (▲). Solid curve is calculated from parameters in Table I for the zinc-blende structure. Dashed curve is calculated for $E_1 = 2.4$ eV. The low-temperature data exhibit impurity scattering. High-temperature data suggest that the larger deformation potential shown in Table I is more accurate than the lower value calculated from Eq. (11).

for the larger deformation potential. Multivalley conduction does not appear to be a complicating factor here as it is in Fig. 4 since no abrupt change in *slope* of the data versus temperature is evident.

In conclusion, it appears that discrepancies between theory and experiment at high temperatures can be removed partially by the inclusion of conduction-band nonparabolicity but mainly by use of *consistently* higher deformation potentials than those calculated from Eq. (11). More high-temperature experiments such as those by Smith[24, 24a, 33] would be helpful in this area. Also needed are detailed measurements of the dependences of the high- and low-frequency dielectric constants upon temperature, especially at high temperatures. The accuracy of the present assumption of temperature-independent dielectric constants could be estimated through Eq. (2). Finally, it appears that the effective masses calculated from Kane's theory[6] by Kurik[20] are sufficiently accurate in cases where careful comparisons with experiment are possible.

ACKNOWLEDGMENTS

F. T. J. Smith graciously provided the author with discussions of high-temperature mobility data. The author recieved the benefit of discussion with A. S. Barker, Jr. and C. H. Henry.

[1]S. S. Devlin, in *Physics and Chemistry of II-VI Compounds*, edited by M. Aven and J. S. Prener (Wiley, New York, 1967), Chap. 11.

[2]R. B. Dingle, Phil. Mag. 46, 831 (1955).

[3]E. Conwell and V. F. Weisskopf, Phys. Rev. 77, 388 (1950).

[4]H. Ehrenreich, J. Phys. Chem. Solids 2, 131 (1957).

[5]H. Ehrenreich, J. Phys. Chem. Solids 9, 129 (1959).

[6]E. O. Kane, J. Phys. Chem. Solids 1, 249 (1957).

[7]N. N. Grigor'ev, I. M. Dykman, and P. M. Tomchuk, Fiz. Tverd. Tela 10, 1058 (1968) [Soviet Phys. Solid State 10, 837 (1968)].

[8]D. L. Rode, Phys. Rev. B 2, 1012 (1970).

[9]M. Aven and B. Segall, Phys. Rev. 130, 81 (1963).

[10]K. Kobayashi, in *II-VI Semiconducting Compounds*, edited by D. G. Thomas (Benjamin, New York, 1967), p. 755.

[11]J. Bardeen and W. Shockley, Phys. Rev. 80, 72 (1950).

[12]J. D. Zook, Phys. Rev. 136, A869 (1964).

[13]J. M. Ziman, *Electrons and Phonons* (Oxford U.P., London, 1967).

[14]S. A. Baron and D. L. Rode have measured $\partial \ln \mathcal{K}_\infty / \partial T$ in CdS, CdTe, and GaAs by an interferometric technique. The results are quoted in the text.

[15]B. Segall, M. R. Lorenz, and R. E. Halsted, Phys. Rev. 129, 2471 (1963).

[16]M. Saitoh, J. Phys. Soc. Japan 21, 2540 (1966).

[17]B. Ray, *II-VI Compounds* (Pergamon, New York, 1969).

[18]D. Berlincourt, H. Jaffe, and L. R. Shiozawa, Phys. Rev. 129, 1009 (1963).

[19]H. Fujita, K. Kobayashi, and T. Kawai, J. Phys. Soc. Japan 20, 109 (1965).

[20]M. V. Kurik, Phys. Letters 24, A742 (1967).

[21]H. Frohlich, Advan. Phys. 3, 325 (1954).

[22]D. Pines, in *Polarons and Excitons*, edited by C. G. Kuper and G. D. Whitfield (Plenum, New York, 1963).

[23]A. S. Barker, Jr. and C. J. Summers, J. Appl. Phys. 41, 3552 (1970).

[24]F. T. J. Smith, Solid State Commun. 7, 1757 (1969).

[24a]F. T. J. Smith, Solid State Commun. 8, 263 (1970).

[25]R. S. Crandall, Phys. Rev. 169, 577 (1968).

[26]S. Toyotomi and K. Morigaki, J. Phys. Soc. Japan 25, 807 (1968).

[27]F. J. Blatt, in *Solid State Physics*, edited by F. Seitz and D. Turnbull (Academic, New York, 1957), Vol. 4.

[28]M. Kohler, Z. Physik 126, 495 (1949).

[29]R. A. Burmeister, Jr. and D. A. Stevenson, Phys. Status Solidi 24, 683 (1967).

[30]P. Hoschl and S. Kubalkova, Czech. J. Phys. 18, B897 (1968).

[31]M. Inoue, J. Phys. Soc. Japan 26, 1186 (1969).

[32]F. T. J. Smith, Metallurgical Trans. 1, 617 (1970).

[33]G. W. Ludwig, IEEE Trans. Electron. Devices ED-14, 547 (1967).

[34]F. A. Kroger, Physica 22, 637 (1956).

[35]M. Aven and C. A. Mead, Appl. Phys. Letters 7, 8 (1965).

[36]F. Matossi, K. Leutwein, and G. S. Schmid, Z.

Naturforsch. 21, A461 (1966).
[37]W. E. Spear and P. G. LeComber, Phys. Rev. Letters 13, 434 (1964).
[38]Y. Fukuda and M. Fukai, J. Phys. Soc. Japan 23, 902 (1967).

PHYSICAL REVIEW B VOLUME 2, NUMBER 10 15 NOVEMBER 1970

Dielectric Theory of Impurity Binding Energies. III. Group-III Acceptors in Si and Ge

J. C. Phillips
Bell Telephone Laboratories, Murray Hill, New Jersey 07974
(Received 22 May 1970)

Chemical shifts of ground-state energies and g factors of acceptors X in Si or Ge host crystals are analyzed within the framework of effective-mass theory. The unit cell centered on the impurity is regarded as a unit cell of a hypothetical SiX of GeX crystal. The differences in energy levels of valence and conduction bands of this hypothetical crystal at Γ, X, and L are calculated according to the semiempirical spectroscopic rules developed by Phillips and Van Vechten to describe levels of zinc-blende crystals. These energy differences are compared with those of the host crystal and are used to renormalize effective masses in the impurity unit cell. Rough estimates then show that this approach yields chemical trends in good agreement with experiment and explains several quantitative features of the data that cannot be explained by qualitative models based on ionic radii or electronegativity differences.

I. INTRODUCTION

In two preceding papers,[1,2] an analysis of the chemical shifts of ground-state energies of donor impurities in Si, Ge, and GaP has been made based on a spectroscopic theory[3,4] of the covalent bond in tetrahedrally coordinated A^NB^{8-N} semiconductors. Both experiment and theory[5] agree that the effective-mass approximation (EMA) of a point-charge impurity embedded in a dielectric quasicontinuum gives an excellent account of the energies and wave functions of excited states of shallow impurities in semiconductors. However, there is now abundant experimental evidence to show that the EMA fails both quantitatively and qualitatively to account for ground-state energies. Quantitatively there is the obvious point that ground-state energies vary from one donor impurity to another (or from one acceptor impurity to another) in the same host crystal, whereas according to the EMA the binding energies of all states are determined only by properties of the host crystal.

It has been customary[5] to explain these "chemical shifts" in terms of a "central cell correction," the breakdown of the hydrogenic approximation for the effective potential in the atomic cell containing the impurity. This brings us no closer to understanding ground-state energies, but it has the convenient feature of relegating the problem to another discipline which already has its own full quota of unsolved problems. The qualitative value of this classification, however, became doubtful when Hopfield and Thomas[6] discovered that even in III-V semiconductors, isoelectronic impurities (such as N in GaP) could bind electrons and holes although the effective impurity potential was *zero* in the EMA. Thus, the EMA is qualitatively wrong in this case, and it appears that we must face up to the problem of shallow impurity states associated with donors and acceptors as well as isoelectronic impurities or isoelectronic-impurity complexes (e.g., CdO in GaP).[6]

The first point to recognize is that in the presence of a short-range potential only, one would not generally expect to find shallow impurity states. Either the potential is not strong enough to produce any bound states, or else it is likely to produce states with a binding energy which is a significant fraction of the energy gap. In practice, unless the difference in electronegativity is very large (e.g., O in GaP), one usually finds small binding energies comparable to EMA binding energies for donors on acceptors and of the same order of magnitude for isoelectronic complexes.

The explanation[7] for this behavior, which for some time made the EMA appear to be more accurate than it really is, is that because most semiconductors are highly polarizable, a strain field develops around each impurity to prevent the accumulation of electronic charge much above or more below the requirements of the valence bonds of the host lattice.

In the case[1] of shallow donor impurities in Si or Ge, the central cell corrections $\Delta E_d = E_I^d - E_0^d$ do not vary monotonically with impurity size. Here E_I^d is the donor ground-state energy and E_0^d is the EMA ground-state energy. Instead, ΔE_d is found to reach a minimum value at Sb in both Si and Ge host crystals. This suggested to us that one could account[1,2] for the chemical shifts in ΔE_d primarily